J Nanostruct 16(1): 338-352, Winter 2026

RESEARCH PAPER

Preparation and Characterization of Heterogeneous TiO_2/AC Nanocomposite for Photocatalytic Degradation for Organic Malachite Green Dye Removal

Nahlah Jaber Hussein [1], Alaa Jwade Kadum [2], Inam Joudah Radhi [3], Noorhan Ali Hamza [4], Hamida Idan Salman [5], Nooralhuda M. Abdulhussein [6]*

Department of Chemistry, College of Education for Pure Science, University of Karbala, Iraq

ARTICLE INFO

Article History:
Received 27 September 2025
Accepted 22 November 2025
Published 01 January 2026

Keywords:
AC/TiO_2 nanocomposite
Heterogeneous
MG Dye
Photo -catalyst
XRD

ABSTRACT

The design and development of novel photocatalysts for treating toxic substances such as industrial waste, dyes, pesticides, and pharmaceutical wastes remain a challenging task even today. To this end, a biowaste pistachio-shell-derived activated carbon (AC) loaded TiO_2 (/AC TiO_2) nanocomposite was fabricated and effectively utilized towards the photocatalytic degradation of Malachite Green dye (MG) under UV-A light. The synthesized materials were characterized for their structural and surface morphology features through various spectroscopic and microscopic techniques, including field emission scanning electron microscope (FE-SEM) along with Energy Dispersive X-ray dispersive spectroscopy (EDX), diffuse reflectance spectra (DRS), X-ray diffraction (XRD), Fourier-transform infrared spectroscopy (FTIR). The presence of AC influences the photocatalytic activity of TIO_2/AC nanocomposite towards MG 100 minutes degradation. These results demonstrate that TIO_2/AC nanocomposite could be effectively used as an ecofriendly, cost-effective, stable, and highly efficient photo- catalyst.

How to cite this article
Hussein N., Kadum A., Radhi I. et al. Preparation and Characterization of Heterogeneous TiO_2/AC Nanocomposite for Photocatalytic Degradation for Organic Malachite Green Dye Removal. J Nanostruct, 2026; 16(1):338-352. DOI: 10.22052/JNS.2026.01.030

INTRODUCTION

The massive levels of pollutants released into water sources worldwide due to increased population expansion and industrial development have generated adverse environmental effects in recent decades. The effluents from textile industries, particularly synthetic dyes, discharged without proper treatment and management adversely affect our environment in one way or another. Moreover, synthetic dyes, present in many industrial wastewaters, are highly stable molecules and are difficult to degrade by conventional physicochemical processes [1]. The dyes are organic soluble compounds, classified as bases, acids, reactive, and directly applied. The ability to fix color in a material is attributed to auxotrophic groups, which are polar and can bind to polar groups of textile fibers; however, this capability is not always present [2]. Malachite green (MG) is a well-known synthetic dye used in the textile industry, in the paper dyeing process, and as a food coloring agent. It is a triphenylmethane cationic dye, environmentally recalcitrant, and extremely toxic to a variety of aquatic and terrestrial mammals, being carcinogenic and a multi-organ toxin for humans,

* *Corresponding Author Email: anaam.j@uokerbala.edu.iq*

and considered an endocrine-disrupting dye. Despite being banned in several countries, it is still extensively used in the aquaculture industry, i.e., as a fungicide and for protozoan infections in fish. Thus, the removal of dyes, such as malachite green, from wastewater is an important challenge for society, and the subject of several studies over the last few years [3]. Activated carbon is a carbonaceous material often derived from agricultural waste. Physical and chemical methods used to synthesize activated carbon. Activated carbon has attracted significant attention in various fi elds due to its excellent, chemical, thermal and electrical properties. Titanium dioxide (TiO_2) is an n-type semiconductor, that is widely used as a photocatalyst due to its good thermal stability, low cost, non-toxic, and environmentally friendly properties [4]. Titanium dioxide occurs naturally in many sands and rocks. TiO_2 is a semiconductor material that can be activated by light using a band gap value of 3.2 eV. The main drawback of titanium dioxide nanoparticles is their easy agglomerated, poor absorption capacity and high electron-hole reprocessing rate.An increase in the recombination rate reduces the degradation efficiency of the nanocatalyst [5].

Heterogeneous photocatalysis is considered one of the most promising processes for wastewater treatment, given its potential for complete mineralization of pollutants to non-toxic products. It implies using a semiconductor that is excited by UV or visible light, being the created electron/hole pairs responsible for the redox reactions that lead to the pollutant's degradation. Many semiconductors, such as ZnO, CuO, Ga_2O_3, have succeeded to be suitable as photocatalysts,

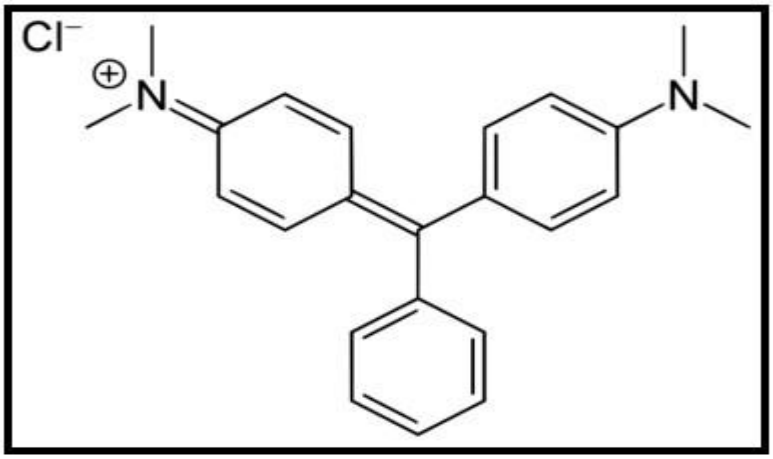

Fig. 1. Chemical Structure of Malachite Green (MG) [17].

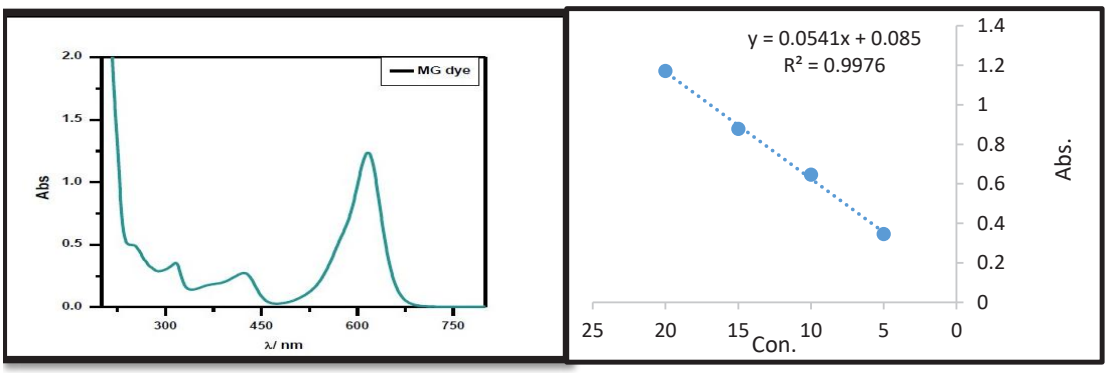

Fig. 2. A-UV-Visible absorption spectra of Malachite green (MG) dye, and B- Calibration curve for MG dye.

and titanium dioxide (TiO_2) is among the preferred ones because of its high chemical stability and low cost, being environmentally friendly. Heterogeneous photocatalysis is not only suitable for the oxidation of organic compounds, but also for the inactivation of microorganisms. However, it also has some drawbacks, such as the high rate of electron/hole (e^-/h^+) pairs recombination, and the hard sedimentation and difficult separation in liquid processes, given its small particle size. Improving the TiO_2 efficiency is, for all these reasons, indeed interesting. Titanium dioxide (TiO_2) is a naturally occurring oxide of titanium. It exists in three crystalline phases, namely, brookite, anatase and rutile. The rutile phase is thermodynamically stable compared to the anatase and brookite phases, which are metastable. The advantages of TiO_2 are that it effective, contains electrochemical properties and is safe to produce. In addition, TiO_2 possesses antimicrobial and UV-protection properties. Applications of titanium dioxide include the use of a photocatalyst for water-dye degradation, and pharmaceuticals, where adsorbent hydrogel incorporated with TiO_2 nanoparticles was used for removing pollutant from water. The group reported that incorporating TiO_2 nanoparticles improved the recovery of the hydrogel from the aqueous solution after the removal of pollutant, also hydrogel was modified with TiO_2 for antimicrobial activity, Therefore, looking at these properties, the TiO_2 would be ideal for preparing hydrogels for adsorbing pollutant [6]. Titanium dioxide exist in three crystalline phases: rutile, anatase, and brookite. The anatase structure has a band gap energy of 3.2 eV and absorbs ultraviolet radiation. The rutile structure has a band gap of 3.0 eV and absorbs ultraviolet rays, as well as radiation that is slightly closer to the visible spectrum. The third structure, brookite, has a band gap of 2.96 eV and absorbs wavelengths close to the visible spectrum. The brookite structure is not used in industrial applications [7,8] Both rutile and anatase structures can be described in terms of chains of TiO_6 octahedral, where each Ti^{+4} ion is surrounded by an octahedron of six O^{-2} ions. It is a surface phenomenon that arises from the accumulation of a large number of particles in the form of molecules, atoms or ions and is called the adsorbent on the surface or interface of a substance in the solid or liquid phase and is called the adsorbent substance. The adsorption process arises due to the presence of unbalanced forces [10], and adsorption leads to the saturation of the fields of these forces present on the surface, and thus this causes a decrease in the free energy ΔG of the surface, i.e. the adsorption process is automatic with the decrease in the degrees of freedom of the adsorbed substance, which is expressed thermodynamically by the decrease

Fig. 3. Real image of photos demonstrates the effectiveness of the photocatalytic process MG dye.

in entropy ΔS, for her. Because the park particles are restricted due to their connection to the diamond surface, and as a result, they lose their freedom of movement and become less random [11]. There are factors that affect the adsorption process, including the nature of the adsorbent, the surface area, the effect of the acid function, the temperature, and also the concentration of the adsorbent.[13]. In this study, A relation between the amount of adsorbate adsorbed on a given surface at constant temperature and the equilibrium concentration of the substrate in contact with the adsorbent is known as adsorption Isotherm.TiO_2/AC nanocomposites were characterized using field emission scanning electron microscope (FE-SEM) along with Energy Dispersive X-ray dispersive spectroscopy (EDX), X-ray diffraction (XRD), Fourier-transform infrared spectroscopy (FTIR). Indeed, our work lies in the unique combination of TiO_2/AC nanocomposites and MG dye type, which has not been explored in previous studies.

MATERIALS AND METHODS

Materials

The study's chemical materials were procured from commercial sources and were utilized unpurified. Commercial P_{25} (Aeroxide) titanium dioxide was provided by Alpha Chemika. Activated carbon was purchased from Sigma-Aldrich. Malachite Green Dye [($C_{23}H_{25}C_lN_2$), and molecular weight (364.9 g/mol)], and sodium hydroxide (NaOH, 99%).

Preparation of TiO_2 doped AC nanocomposite

The TiO_2/AC NPs were created by dissolving 2 g of commercial TiO_2 in 100 mL of distilled water (DW). The mixture was then slowly added 1 M sodium hydroxide until the pH of the solution reached 8.5 while being constantly agitated with a magnetic stirrer for 3 hours. After that, a certain quantity of activated carbon (AC) was added to the solution mentioned above, and it was agitated for four hours at 60 °C. Centrifuge was used for 60 minutes at 3000 rpm to separate the resultant precipitate. Following a 4-hour vacuum oven drying process at 80 °C, the precipitate was further calcined in air for 1.5 hours at 350 °C.

Preparation of Malachite Green dye solution

Malachite green is an organic compound that is used as a dyestuff and controversially as an

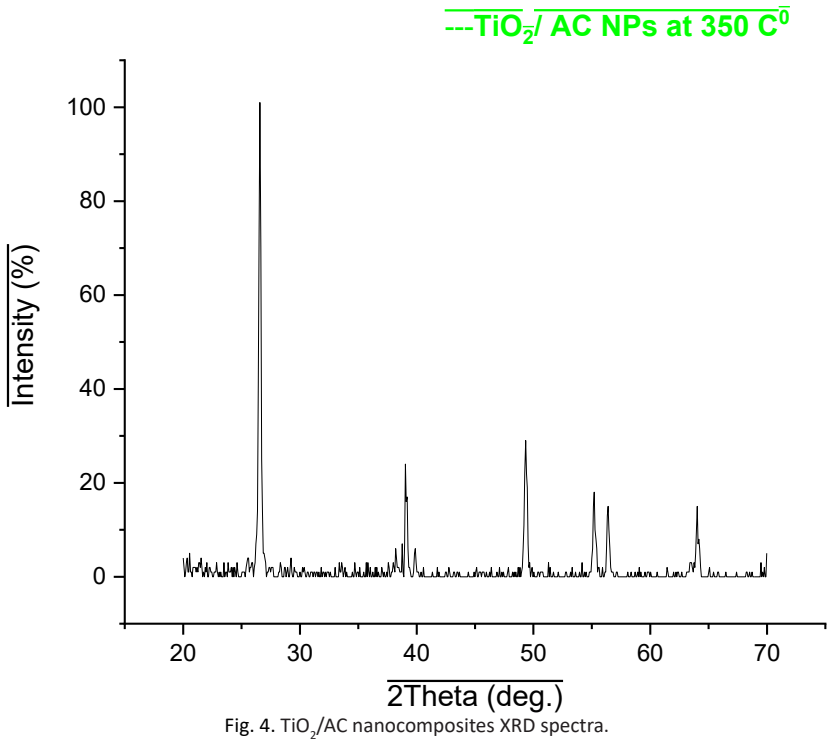

Fig. 4. TiO_2/AC nanocomposites XRD spectra.

antimicrobial in aquaculture. So, the chemical structure of Malachite Green (MG) was shown in Fig. 1. Malachite green is traditionally used as a dye for materials such as silk, leather, and paper. Despite its name the dye is not prepared from the mineral malachite; the name just comes from the similarity of color [14]. MG was chosen to study the binary nanocomposite's photocatalytic activity during synthesis activated carbon (AC) loaded TiO_2 (TiO_2/AC) nanocomposite. MG dye, an N-methylated diaminotriphenylmethane dye, is used primarily as a therapeutic agent in aquaculture. In solution, the dye exists as a mixture of the cation (chromatic malachite green) and its carbinol base MG dye is one of the organic compounds that has emerged as a controversial agent in the aquaculture and is used as a dyestuff [15]. For the removal of noxious dyes various treatment methods and materials were applied such as membrane filtration, photocatalyzed degradation, microbiological, oxidation, ozonation, adsorption, coagulation/flocculation, and degradation by biological processes [16].

A Malachite green dye is a very well - known cationic dye that has a molecular formula ($C_{23}H_{25}C_lN_2$), and molecular weight (364.9 g/mol); the dye is odourless green crystals powder used for various purposes. A stock solution (1000 mg L^{-1}) was prepared by dissolving (1.0 g) of MG dye in (1000 mL) distilled water. To determine the maximum wavelength of Malachite green dye. The ultraviolet-visible absorption spectra of MG dye solution was recorded within wavelengths of 200-800 nm. Where the maximum wavelength of the solution was determined from its highest absorption in the UV-Vis spectrum found at the wavelength λmax MG= 624 nm, the wave length absorption as shown in Fig. 2a and the calibration curve for MG dye as shown in Fig. 2b.The beer's law is followed in the concentration range of 20 to 100 ppm [18].The solution was then irradiating for 120 minutes using philips mercury lamp UVT (A) which was placed in a home-made photoreactor as (a) shown in Fig. 3.

Photocatalytic decomposition experiments

Degradation reactions are carried out to assess the produced catalyst's activity. First, we need to ascertain the impact of catalyst loading. The studies were conducted using various catalyst concentrations for dye solutions and dye concentrations (ppm) at room pH. A 250 ml Pyrex glass beaker and a magnetic stirring apparatus with an oxygen bubble source made up the reactor. Above the beaker, the bulb was positioned perpendicularly. There were 15 centimeters separating the Pyrex glass beaker and the lamp. It was found through analysis using a (UV-Visible) spectrophotometer that a centrifuge was required in order to remove the minor amounts of (TiO_2/AC) that were useful. A (UV-Visible) spectrophotometer [(Type Shimadzu, Japan, PC 1650-303, University of Karbala/College of Education for Pure Science-Chemistry Department)] was used to measure the dye concentration. 298 K was the temperature utilized in each test.Aldrich's Green (MGD) dye by Sigma-Malachaite. Since cationic dye models were used to assess photocatalytic performance, TiO_2/AC NPS was distributed in an aqueous dye solution containing 20 ppm. Before the suspension was subjected to radiation, it was magnetically agitated for 90 minutes in the dark to bring the

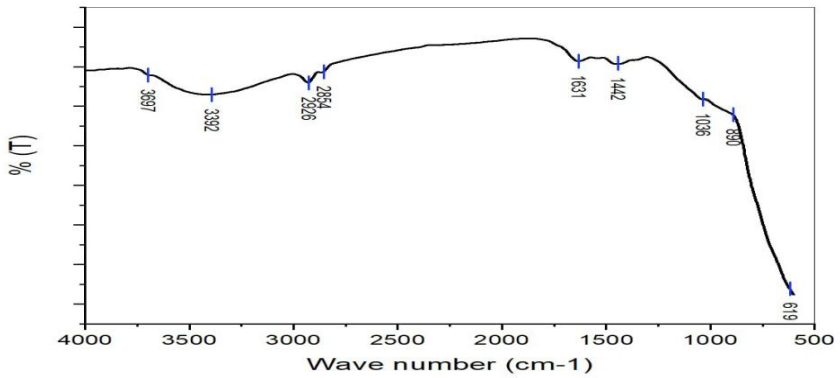

Fig. 5. FTIR of TiO_2/AC nanocomposites

dye's adsorption and desorption processes into balance. Approximately five milliliters of sample were obtained throughout each of the fifteen minutes of testing. The aqueous solution was centrifuged to remove any suspended solid particles. Using distilled water as a reference, the residual dye concentration in a MG dye solution contained in a micro-cuvette was measured at 624 nm using a UV-visible spectrophotometer, see Fig. 2. The degradation efficiency was calculated using the following equation. The degradation efficiency was calculated using the following Eq. 1.

$$\text{Photo Decomposition Efficiency (PDE) (\%)} = \frac{C_0 - C_t}{C_0} \times 100$$

Where C_o: is the dye concentration at the start of the test, and C_t: is the dye concentration following a period of testing (t). The pseudo-first-order kinetic model (Eq. 2) was employed to investigate the organic dye's photocatalytic degradation kinetics in the presence of the photocatalysts.

$$\ln(C_0/C_t) = kt$$

Where t is the time interval, k is the rate constant, and C_0 and C_t are the model dye's concentrations before and after radiation, respectively. The rate constant can be found by sloping the plot of $\ln(C_0/C_t)$ vs. t [19].

RESULTS AND DISCUSSION

Characterization of loaded TiO_2 on Activated Carbon nanoparticles

The XRD pattern of TiO_2/AC NPs is shown in Fig. 4. The diffraction peaks at 28°, 38°, 50°, 55°, 56°, and 64° here were all in good agreement with the anatase phase of TiO_2/AC. No additional summits suggest the existence of impurities due to the influence of calcination (350 C°). (JCPDS card no. 21-1272) The diffraction peaks seem to have a clear, crisp crystal form. The following method was used to measure the TiO_2/AC nanocomposite's crystallite size: Debye - Scherrer's [20].

$$\text{Crystalline size (D)} = \frac{K\lambda}{\beta\cos\theta}$$

Where λ is the wavelength of the Cu-Kα X-ray (λ

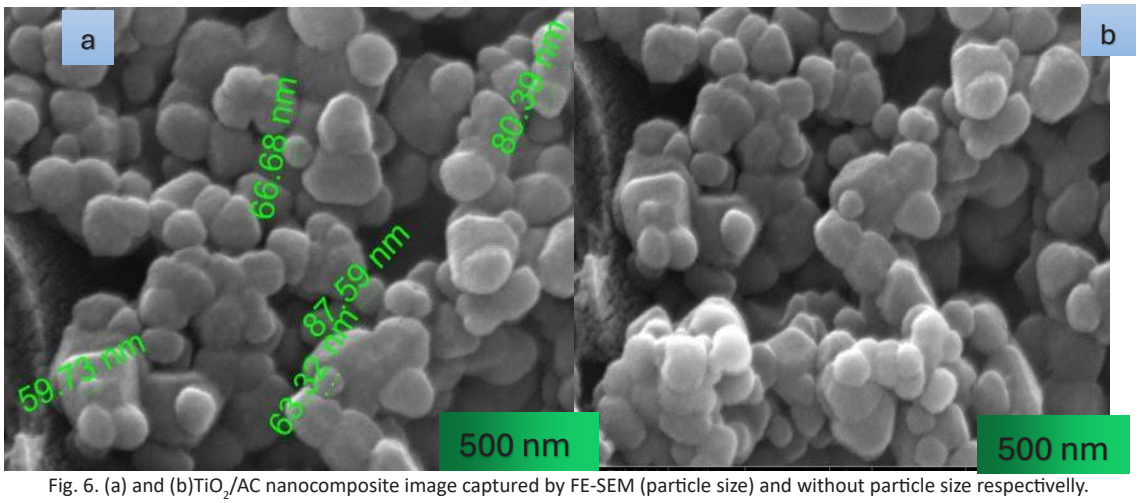

Fig. 6. (a) and (b)TiO_2/AC nanocomposite image captured by FE-SEM (particle size) and without particle size respectivelly.

Table 1. TiO_2/AC nanocomposites' composition was examined using EDX.

Sample	Ti Atomic %	Na Atomic %	Mg Atomic %	Ca Atomic %	C Atomic %	Au Atomic %	O Atomic %	Al Atomic %
TiO_2/AC NPs	3.7	0.3	0.4	0.2	68.7	3.0	16.2	7.5

= 1.5406 Å), θ is the diffraction angle, and β is the full width at half maximum (in radians). K is the Debye Scherer constant.

The FT-IR measurements were carried out to know the molecules that are responsible for the Fig. 5 shows a significant peaks (2854,2926) cm^{-1} for (C-H, aliphatic), peak (1631) cm^{-1} for (-C=O, asymmetric stretching) and (1442) $cm^{-1}$for (-C=O, symmetric stretching), peaks (2000, 2600) cm^{-1} for O-H, in plane) and (619 cm-1 for O-H , out of plane), peak (1036) cm^{-1} for (C-O), peak(890) cm^{-1} for TiO_2.

Using FE-SEM analysis, the produced materials' average size and surface morphology were determined. Fig. 6 represents the FE-SEM images of prepared TiO_2/AC nanocomposites. The TiO_2/AC needles have an average size and diameter of (71.52) nm. The movement of photoexcited charge carriers on the surface of TiO_2/AC nanocomposites is caused by the flake, spherical, and one-dimensional (1D) needles that can be seen in the FE-SEM picture of the nanocomposites; In the course of the degradation process, it may suppress the rate of electron-hole pair recombination[14]. Using EDX mapping on an EDX microanalysis system, the element distribution of these TiO_2/AC nanocomposites can be found in Fig. 7. The elements Ti, Na, Mg, Ca, C, Au, O, and Al have signals linked to the Map Micrograph Technique (MMT).

The nanocomposites' EDX spectra are displayed in Fig. 7. The TiO_2/AC micrograph also shows some agglomerations, which could be caused by mild electrostatic interactions and polar attraction between the particles. Furthermore, since all of the TiO_2 particles were sintered at a high temperature (350 °C) to guarantee complete crystallization, this behavior may have resulted from particle adhesion. TiO_2/AC NPs showed rough porous architectures and were evenly distributed on the surface of AC, suggesting that the TiO_2/AC nanocomposite was successfully synthesized [21].

The presence of the TiO_2/AC nanocomposite was confirmed by energy dispersive X-ray dispersive spectroscopy, or EDX. The TiO_2/AC nanocomposite nanocrystal line exhibits strong and precise diffraction peaks,indicating good crystallinities. The EDX spectra of the pure TiO_2/AC nanocomposite reveal the presence of only Ti, C, O, and Al. Table 1 provides a semi-quantitative assessment of the atomic concentration (atom%). It indicates that the products' TiO_2/AC elements content is (3.7,0.3, 0.4,0.2,68.7,3.0,16.2 and 7.5) for Titanium (Ti), Sodium (Na), Magnesium (Mg), Calcium (Ca), Carbon (C), Gold (Au), Oxygen (O), and Aluminum (Al).

The EDX results are shown in Fig. 7, where it is evident that the weight ratios of TiO_2/AC NPs were, respectively, 3.7 %, 16.2%, 68.7%, 0.3%,0,4%,7.5% and 0.2 %. The EDX examination showed that the sample contained the necessary phases of Ti and O and that the produced TiO_2/AC NPs were highly pure. Similar Ti, O, and AC ratios that are near to the theoretical values are seen in the EDX results from the current investigation.

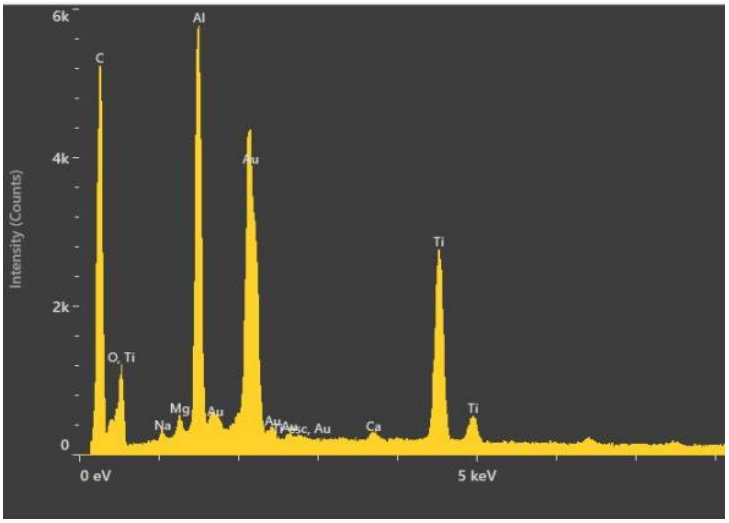

Map sum spectrum of TiO_2/AC NPs

Elemental	Atomic %	Weigh
Ti	3.7	0.1
O	16.2	0.6
C	68,7	0.3
Na	0.3	0.1
Mg	0.4	0.0
Al	7.5	0.1
Ca	0.2	0.0
Au	3.0	0.5

Fig. 7. Pure TiO_2/AC NPs elemental mapping and EDX analysis.

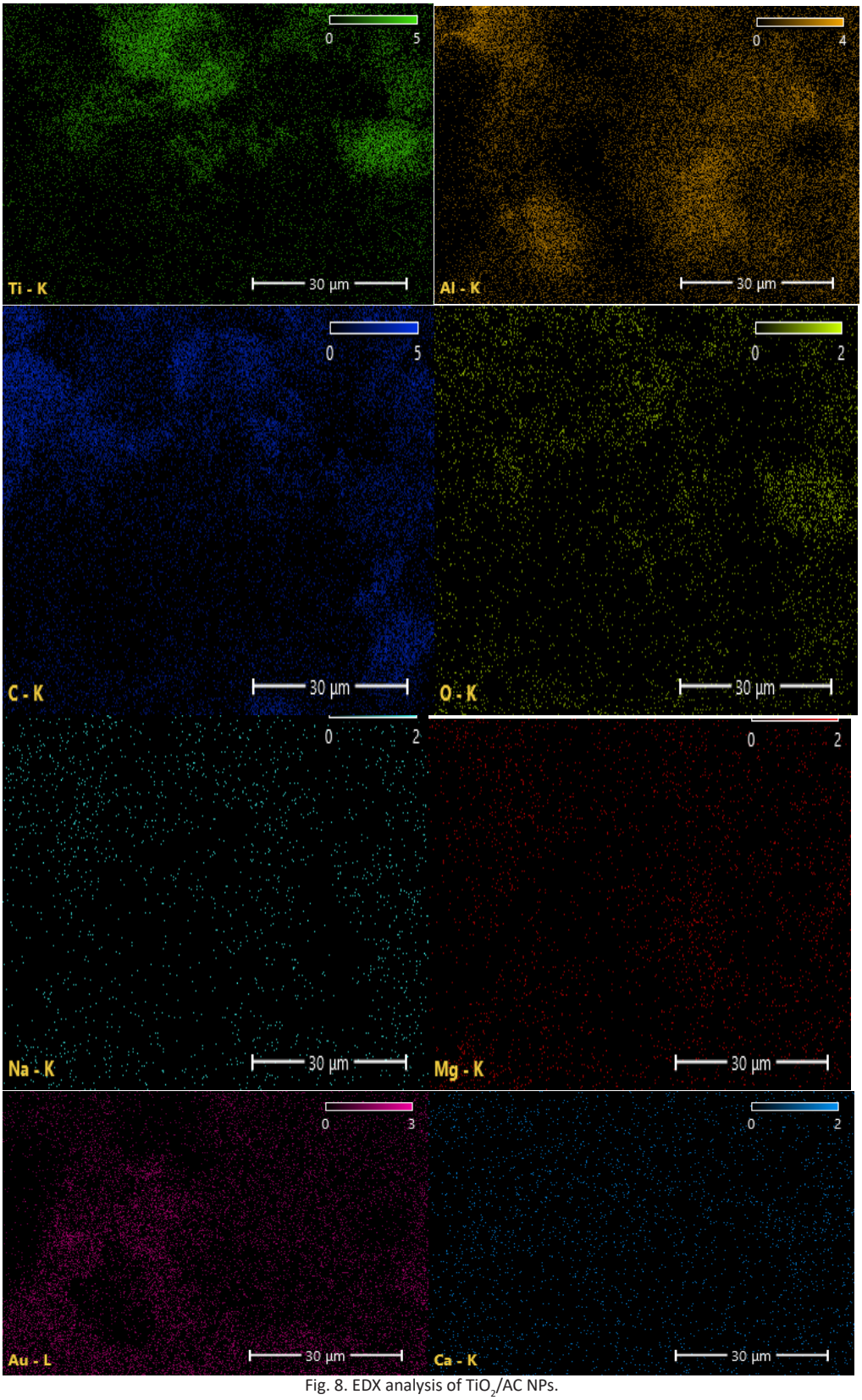

Fig. 8. EDX analysis of TiO_2/AC NPs.

TiO_2/AC NPs samples' chemical composition is revealed by EDX analysis. The produced samples are mostly made up of Ti, O, C, Na, Mg, Al, Ca, and Au, with very little Mg and Ca present, as shown in Fig. 8.

Influence of various TiO_2/AC nanocomposites photodeposition process parameters on MG dye

Effect of mass dosage

Impacts of a photocatalyst concentration of (0.2,0.4,0.6,0.8) gram on the (MG) dye photocatalytic degradation at reaction temperatures of 25 °C for (1) hour. It is possible to assess the experimental results under the assumption, as shown in Figs. 9a and b. A pesudo first order kinetic model was used to discuss the findings [10]. The impact of catalyst surface mass (TiO_2/AC) nanocomposites on the dye photodegradation process is depicted in Fig. 9. Due to this factor, all settings must stabilize (25) ppm for dye concentration and 1.71 mW/cm2 for light intensity. After that, the catalyst surface (TiO_2/AC) nanocomposite and green dye solution were combined, and the mixture was stirred for 100 minutes under UVA light (using a UVA LED lamp). Following that, the supernatant was separated by centrifugation at 150 rpm, and the concentration that remained was determined using a UV-visible spectrophotometer set to 624 nm in wavelength.

When (TiO_2/AC) NPs are added in an increment of 0.2 gm to 0.8 gm, the photocatalytic efficiency increases from 50% to 97% in (1) hour. The number

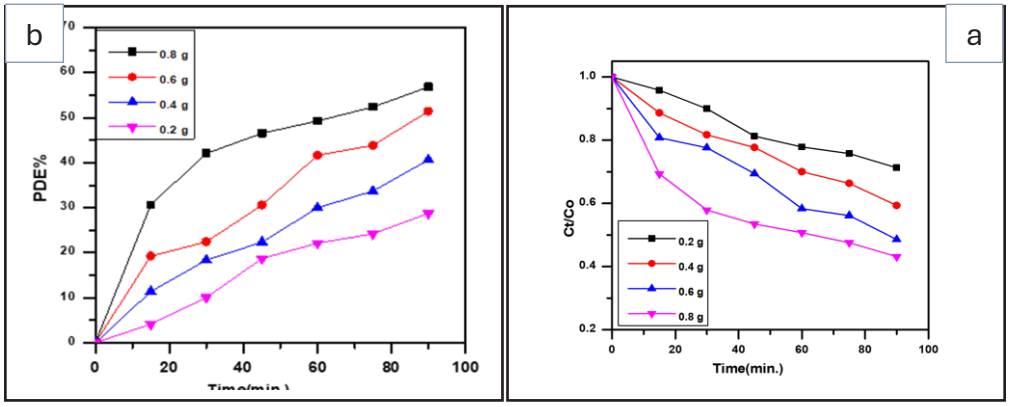

Fig. 9. (a)At mass dosage of (0.2,0.4,0.6,0.8) gm on the photocatalytic degradation of MG dye produced, and (b) The efficiency PDE % of various mass dosages on the photocatalytic degradation of MG dye.

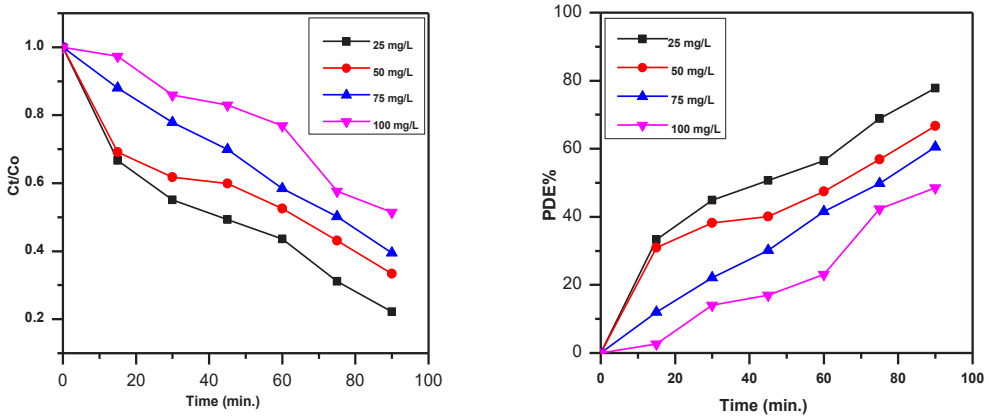

Fig. 10. (a) The effect of TiO_2/AC NPs at concentrations of 25–50–75–100 ppm on the photocatalytic degradation of MG dye generated; and (b) PDE % the effectiveness of MG dye concentration.

of active sites on the catalyst surface increased due to an increase in mass, and this in turn accelerated the pace at which radicals develop [22]. The catalyst weight of 0.2 gm produced the largest decrease in the C/C° value, as shown in Fig. 9a. In contrast, Fig. 9b shows that when the photocatalyst dose was increased from 0.2 to 0.8 gm, respectively, the Photocatalytic degradation efficiency (PDE%) values grew consistently 97%. Overall, the higher MG PDE% was achieved with 0.8 gram of TiO_2/AC photocatalyst. The presence of more active sites on the photocatalyst surface may affect the photocatalytic performance.

Effect of MG dye concentration

Different MG (25-100) ppm concentrations were used in order to examine the effect of the dye's starting concentration upon TiO_2/AC. A bulk dosage of 0.4 gm is displayed in Fig. 10. The main ingredient of the dye solution has a big impact on how quickly MG degrades. The dye's photocatalytic degradation in relation to concentration and duration [23]. The experimental data could be assessed under the assumption of pseudo first order kinetics,as shown in Fig. 10a. To assess the use of the TiO_2/AC nanocomposite surface as a catalyst for the textile pollution-causing dye MG's photodegradation. To examine how the initial concentration of MG dye affected the efficiency of TiO_2/AC NPs, a number of dye concentrations ranging from 25 to 100 ppm were carefully selected. investigated the room temperature photocatalytic breakdown rate of (MG) dye. For (1) hour, the light intensity was 1.71 mW/Cm^2 and the amount of TiO_2/AC was 0.8 gm. See Fig. 10b. Because there are fewer photoactive sites available for the sorption of ^-OH ions required to produce ^-OH radicals, an increase in the initial dye concentration results in the loading of more dye molecules on the photocatalyst surface, which inhibits the formation of OH species.

Therefore, for a given reaction temperature, photocatalyst dose, and illumination period, the production of OH radicals on the photocatalyst surface remains constant due to the unavailability of active sites [24]. At high concentrations (25 and 50 ppm), the OH species that are generated are therefore inadequate

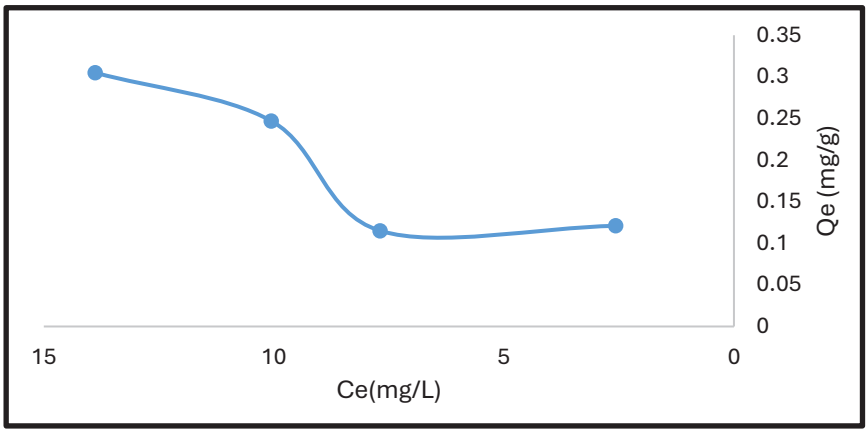

Fig. 11. Adsorption isotherms of malachite dye on the surface of titanium oxide at a temperature of 298 K.

Table 2. Ce and Qe values in the adsorption of malachite dye on the surface of titanium oxide at a temperature of 298 K.

C	Ce	Qe
5	2.569	0.121
10	7.689	0.115
15	10.055	0.247
20	13.881	0.305

for the photocatalytic destruction of MG dye. Additionally, because of the potential for dye molecule aggregations at high concentrations, PDE% may be impacted by limitations on light penetration and/or absorption. These findings demonstrate that photocatalytic degradation of MG dyes adheres to a pseudo first order kinetic model[25].

Effect of different parameters of adsorption processes of TiO_2/AC nanocomposites onto Malachite Green dye

Adsorption isotherms

The malachite dye was adsorbed, and the adsorption isotherms were obtained at 298 K, as shown in Table 2 and Fig. 11. It is clear from the drawing that the general shape of the adsorption isotherms is of the S^2 type, according to the Giles classification, which goes back to the Freundlich principles of adsorption. This indicates that the surface of the adsorbent is a heterogeneous surface, and also when the covered part of the adsorbent surface increases, the temperature of adsorption will decrease. The increasing shape of the isotherm with increasing equilibrium concentration confirms that the arrangement of the molecules on the surface is horizontal on the surface and the adsorption is monolayer,and that the interaction of the adsorbed material with the adsorbent surface takes place through hydrogen bonding forces [23]. The malachite dye adsorption data were treated according to the linear form of the following Freundlich logarithmic equation:

$$\log Q_e = \log K_f + \frac{1}{n}\log C_e$$

The effect of acid function on the adsorption isotherm of malachite dye on the surface of titanium oxide

The effect of the acid function on the adsorption of malachite dye to the surface of titanium oxide was studied at different acidity values (pH = 2, 4, 8). The results were shown in Table 5 and Fig. 14, where it increases when it is less basic at (pH = 8). And it decreases The amount of adsorption when the medium is acidic (pH = 4) and decreases more when the medium is more acidic (pH = 2) as shown in the following order: - pH= 10 >4 >2.

The explanation for this is that the increase in the amount of adsorption in the basic medium is the result of the spread of the positive charge on

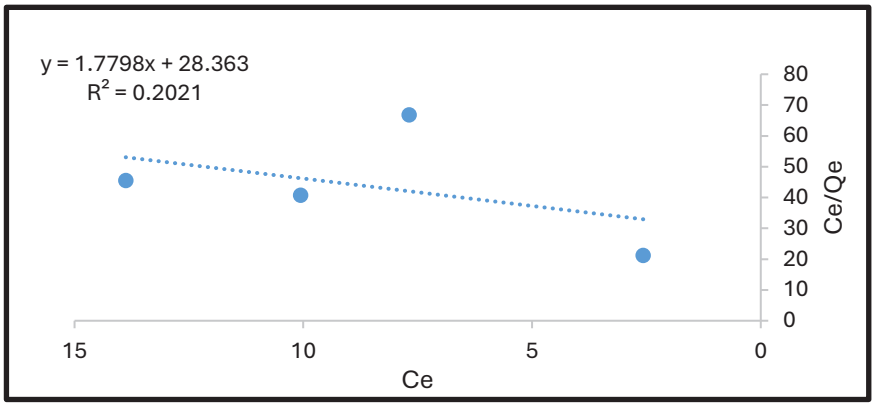

Fig. 12. Freundlich rectifiers for adsorption of malachite dye on the surface of titanium oxide.

Table 3. Logarithm values of Qe and Ce for malachite dye at a temperature of 298 K.

C	Log Ce	Log Qe
5	0.409	-0.917
10	0.885	-0.949
15	1.002	-0.607
20	1.142	-0.515

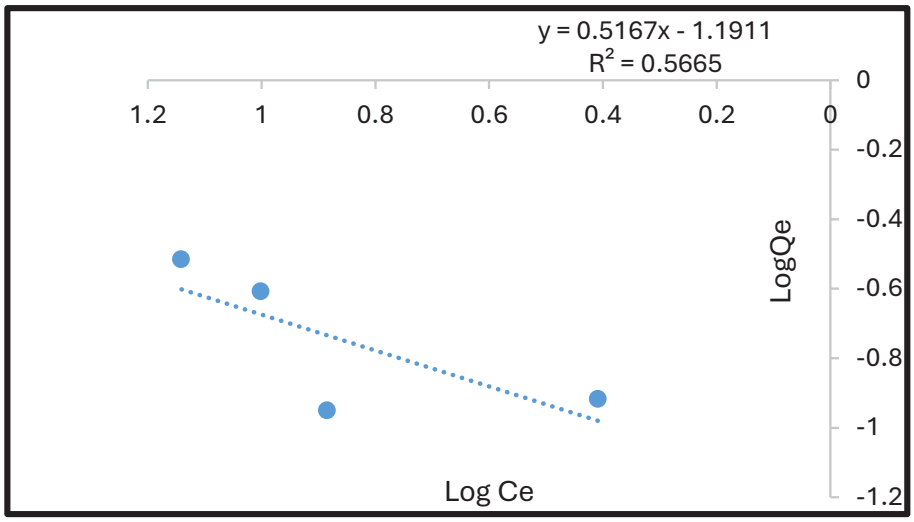

Fig. 13. Lankmeier rectifiers for the adsorption of malachite dye on the surface of titanium oxide.

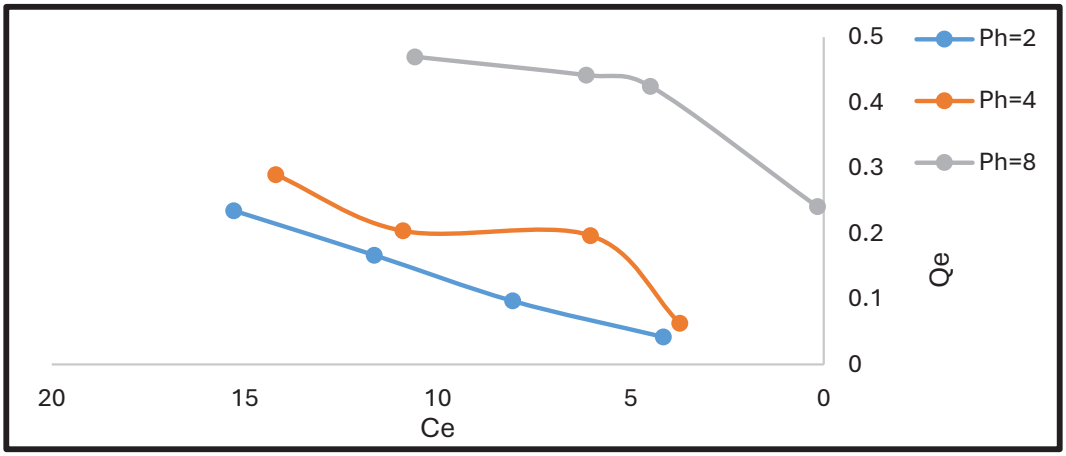

Fig. 14. The effect of the acidity of the solution on the adsorption of malachite dye onto the surface of titanium oxide at a temperature of (298 K).

Table 4. shows the adsorption of malachite dye on the surface of titanium oxide at a temperature of 298 K.

C	Ce	Ce/Qe
5	2.569	21.231
10	7.689	66.86
15	10.055	40.708
20	13.881	45.511

the surface, and this works to increase the amount of adsorption. Also, the dye medium is acidic, so the amount of adsorption in the acidic medium decreased and increased in the basic medium [24].

Calculating the values of the thermodynamic functions ΔG, ΔH, ΔS

The values of the thermodynamic functions represented by ΔGad, ΔHad, and ΔSad were calculated, where Δ H was calculated by drawing the relationship between (LoXm) versus the reciprocal of temperature (1/T), and their values are shown as in Table 6, based on Vant-Hoff-Arrhenius Equation [26].

$$\log X_m = \left(\frac{-\Delta H}{2.303RT}\right) + Cons$$

It represents: Log Xm: logarithm of the highest amount adsorbed (mg/g) .

R: the general gas constant.

T: temperature.

K: Cons: constant of the van't Hoff equation.

A linear relationship was obtained and the slope of this relationship was as shown in Fig. 15. Then the value of ΔH was calculated, and the slope is equation:

$$\Delta G = -RT \ln \frac{Q_e}{C_e}$$

When applying the Gibbs equation [27], we obtain the values of the entropy change (ΔS) as shown in Table 6, and this is the Gibbs equation.

$$\Delta G = \Delta H - T\,\Delta S$$

Table 7 shows the values of (ΔG ad, ΔHad, ΔSad)

Table 5. The effect of the acidity of the solution on the adsorption of malachite dye to the surface of titanium dioxide at a temperature of 298 K.

C	pH=2		pH=4		pH=8	
	Ce	Qe	Ce	Qe	Ce	Qe
5	4.158	0.042	3.733	0.063	0.166	0.241
10	8.059	0.097	6.044	0.197	4.491	0.425
15	11.645	0.167	10.905	0.204	6.155	0.442
20	15.286	0.235	14.195	0.290	10.591	0.470

Table 6. shows the values of 1/T and Log Xm for malachite dye within the experimental temperature range (298 – 318 K).

T(K)	1/T	LogXm
298	0.00304	-0.198
308	0.00314	-0.29
318	0.00324	-0.425
328	0.00335	-0.515

Table 7. shows the values of (ΔG ad, ΔHad, ΔSad) for the malachite dye on the surface of titanium oxide at a temperature of 298 K.

T(K)	ΔG J/mol	ΔHJ/mol	ΔSJ/mol.K
298	-9459.28	19625.82	97.601
308	-8978.11		92.8699
318	-7791.17		86.2194
328	-6683.85		80.2123

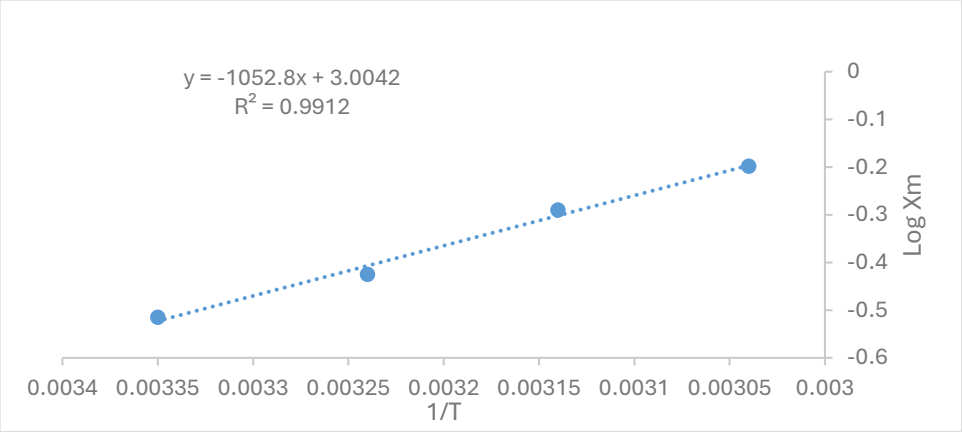

Fig. 15. Relationship between Log XmAnd the reciprocal of the temperature (1/T) for the adsorption of malachite dye on the surface of titanium oxide.

for the malachite dye on the surface of titanium oxide at a temperature of 298 K.

Negative values of free energy (ΔG) indicate that adsorption on the TiO_2 surface is (spontaneous) under experimental conditions. As for the positive values of ΔH) indicate that the adsorption process on the surface of TiO_2 is endothermic [28], as the adsorption increases with increasing temperature, and it also indicates an increase in the exchange between the adsorbent surface and the adsorbed material with increasing temperature. Positive (ΔS) values indicate that the adsorbed molecules are random than they are in the solution when the adsorption process and the absorption process occur at the same time [29].

CONCLUSION

The photocatalyst of TiO_2 activated carbon composite (TiO_2/AC) used in this study was made economically and at a reasonable cost using the precipitated technique.as well as other related factors like effect mass dose and concentration. According to the catalyst's characterization, TiO_2 was evenly distributed across the surface of the activated carbon. The XRD, FTIR, FESEM, and EDX methods verified the effective synthesis of nanomaterials. According to the results of photocatalysis degradation for MG dye, the TiO_2/AC nanocomposite exhibited higher activity (PDE%= 97). The photocatalytic degradation reaction adheres to the pseudo first order paradigm, as demonstrated by the kinetic analysis. The produced composite material is therefore very useful for the treatment of wastewater from the environment and the elimination of dye. The results showed that the reaction was endothermic, the acid value was as high as possible in the basic environment, and that the reaction was regular and non-spontaneous.

CONFLICT OF INTEREST

The authors declare that there is no conflict of interests regarding the publication of this manuscript.

REFERENCES

1. Alghamdi YG, Krishnakumar B, Malik MA, Alhayyani S. Design and Preparation of Biomass-Derived Activated Carbon Loaded TiO2 Photocatalyst for Photocatalytic Degradation of Reactive Red 120 and Ofloxacin. Polymers. 2022;14(5):880.
2. Mittal M, Sharma M, Pandey OP. UV–Visible light induced photocatalytic studies of Cu doped ZnO nanoparticles prepared by co-precipitation method. Solar Energy. 2014;110:386-397.
3. Boumad S, Cano-Casanova L, Román-Martínez MC, Bouchenafa-Saib N, Lillo-Ródenas MA. Removal of malachite green from water: Comparison of adsorption in a residue-derived AC versus photocatalytic oxidation with TiO_2 and study of the adsorption-photocatalysis synergy. Environ Res. 2024;250:118510.
4. Baldrian P, Merhautová V, Gabriel J, Nerud F, Stopka P, Hrubý M, et al. Decolorization of synthetic dyes by hydrogen peroxide with heterogeneous catalysis by mixed iron oxides. Applied Catalysis B: Environmental. 2006;66(3-4):258-264.
5. Singh P, Vishnu MC, Sharma KK, Borthakur A, Srivastava P, Pal DB, et al. Photocatalytic degradation of Acid Red dye stuff in the presence of activated carbon-TiO_2 composite and its kinetic enumeration. Journal of Water Process Engineering. 2016;12:20-31.

6. Almeer Kareem FA, Salman HI. Water purification from the anion CO3-2 using (Zn/Al) di layers hydroxide. AIP Conference Proceedings: AIP Publishing; 2023. p. 050035.
7. Anad MF, Salman HE, Al-Baiati MN. Synthesis a novel nano graft co-polymer and studying the swelling behaviors using different molar ratios of acrylic acid monomer. IOP Conference Series: Materials Science and Engineering. 2019;571(1):012096.
8. Eyring H. Physical Chemistry of Surfaces. Arthur W. Adamson. Interscience (Wiley), New York, ed. 2, 1967. xx + 747 pp., illus. $15. Science. 1968;160(3824):179-179.
9. Ece MŞ. Synthesis and characterization of activated carbon supported magnetic nanoparticles (Fe O4/AC@SiO @ Sulfanilamide) and its application in removal of toluene and benzene. Colloids Surf Physicochem Eng Aspects. 2021;617:126231.
10. Hussein FM, Salman HE, Balakit AA. A cross-linked chitosan-Schiff base: new material for the removal of methyl orange from aqueous solution. Desalination and Water Treatment. 2021;234:288-298.
11. Yass DA, Abbas AM. Adsorption of Congo Red Dye on Activated Graphite and Its Composite, An Isothermal and Thermodynamic Study. Azerbaijan Chemical Journal. 2025;0(2):70-78.
12. Qian D, Bai L, Wang Y-S, Song F, Wang X-L, Wang Y-Z. A Bifunctional Alginate-Based Composite Hydrogel with Synergistic Pollutant Adsorption and Photocatalytic Degradation Performance. Industrial & Engineering Chemistry Research. 2019;58(29):13133-13144.
13. Robati D, Rajabi M, Moradi O, Najafi F, Tyagi I, Agarwal S, et al. Kinetics and thermodynamics of malachite green dye adsorption from aqueous solutions on graphene oxide and reduced graphene oxide. J Mol Liq. 2016;214:259-263.
14. Bedour Ali M, Inam Joudah R. Study the characterization and preparation of silver nanoparticle using friendly green synthesis. Journal of the Pakistan Institute of Chemical Engineers. 2024;52(1).
15. Kayranli B. Adsorption of textile dyes onto iron based waterworks sludge from aqueous solution; isotherm, kinetic and thermodynamic study. Chem Eng J. 2011;173(3):782-791.
16. Mashkour MS, Kahlol MK, Al-Hasnawi SW. Colorimetric Determination of Metoclopramide Hydrochloride and Glutathione by using 1,2 Naphthaquinolinc-4-Sulphonate Sodium Reagents. Research Journal of Pharmacy and Technology. 2018;11(8):3290.
17. Machado Garcia R, Carleer R, Arada Pérez M, Puente Torres J, Gu Y, Samyn P, et al. Fe-TiO_2/AC and Co-TiO_2/AC Composites: Novel Photocatalysts Prepared from Waste Streams for the Efficient Removal and Photocatalytic Degradation of Cibacron Yellow F-4G Dye. Catalysts. 2021;11(10):1137.
18. Irfan MZ, Qamar S, Saeed U, Ali M, Aleem W, Qamar N, et al. Removal of nickel ions from aqueous solution using treated rice husk: an adsorption study. Journal of the Pakistan Institute of Chemical Engineers. 2023;50(2).
19. Wakkel M. Efficient adsorbent based on pomegranate peel for pollutants removal from aqueous solution. Sustainable Applications of Pomegranate Peels: Elsevier; 2025. p. 151-190.
20. Nidhishree MS, Milind PD, Hiral MM, Swati P, Sunil HC, Sandip VB. Author response for "Kinetic study of adsorption and photocatalytic degradation of methylene blue dye using TiO_2 nanoparticles with activated carbon". IOP Publishing; 2024.
21. Zhu S, Huang X, Ma F, Wang L, Duan X, Wang S. Catalytic Removal of Aqueous Contaminants on N-Doped Graphitic Biochars: Inherent Roles of Adsorption and Nonradical Mechanisms. Environmental Science & Technology. 2018;52(15):8649-8658.
22. Bhat SA, Zafar F, Mondal AH, Kareem A, Mirza AU, Khan S, et al. Photocatalytic degradation of carcinogenic Congo red dye in aqueous solution, antioxidant activity and bactericidal effect of NiO nanoparticles. Journal of the Iranian Chemical Society. 2019;17(1):215-227.
23. Albo Hay Allah MA, Alshamsi HA. Facile green synthesis of ZnO/AC nanocomposites using Pontederia crassipes leaf extract and their photocatalytic properties based on visible light activation. Journal of Materials Science: Materials in Electronics. 2023;34(16).
24. Sireng K. Fish bladder-based activated porous carbon/Co_3O_4/TiO_2 composite electrodes for supercapacitors: The Nelson Mandela African Institution of Science and Technology.
25. Ghazi HH, Aljeboree AM. Synthetic Water-Gel Crystals (Orbeez Balls) as Environmentally Friendly Adsorbent for Removal of Toxic Brilliant Green Dye from Aqueous Solutions. Asian Journal of Water, Environment and Pollution. 2024;21(3):53.
26. Kadhim MA, Salman HE, Ali HaA. Adsorption of Albumin and Creatinine on ZnO Nanoparticles. International Journal of Pharmaceutical Quality Assurance. 2019;10(04):689-695.
27. Rahman MM, Ihara H, Takafuji M. Nanomaterial Hybridized Hydrogels as a Potential Adsorbent for Toxic Remediation of Substances from Wastewater. Recent Trends in Wastewater Treatment: Springer International Publishing; 2022. p. 365-393.
28. Kh. Utilization from Cement Kiln Dust in Removal of Acid Dyes. Am J Environ Sci. 2012;8(1):16-24.
29. Yang H, Wu K, Zhu J, Lin Y, Ma X, Cao Z, et al. Highly efficient and selective removal of anionic dyes from aqueous solutions using polyacrylamide/peach gum polysaccharide/attapulgite composite hydrogels with positively charged hybrid network. Int J Biol Macromol. 2024;266:131213.